

Synchronization of Phasor Measurement Units and its Error Propagation to State Estimators.

Juan A. Bazerque (contact author), Ulises Ribeiro, and Jorge Costa.[†]

Abstract—The recent breakthrough on power grid technologies was promoted by the emergence of phasor measurement units (PMUs), as they provide direct and high-rate data for analyzing and controlling the network. Time becomes critical however, since offsets in the internal clocks of PMUs render their data unreliable. In this context, the present work describes grid-wide implementation of a Precision Time Protocol system to deliver an accurate time reference to PMUs at different power stations. Residual time offsets are modeled as PMU noise, propagating to linear state estimators, and their non-linear counterparts that result from combining PMU and power flow data.

Keywords: Phasor measurement units, synchrophasor, synchronization, Precision Time Protocol, state estimation.

I. INTRODUCTION

The integration of phasor measurement units (PMUs) to power grids around the world constituted a technological breakthrough that triggered research efforts in several directions [1]. In transient stability analysis, PMUs provide the grid control system with voltage and current phase samples per cycle promoting research on new algorithms for the prediction of generators going out-of-step [2]. The traditionally nonlinear state estimation (SE) problem, consisting of finding voltage magnitudes and phases at all buses in the grid, has also been restated, as PMU data relate linearly with the state variables to solve for. One line of research in this direction is to incorporate new PMU data into STE while taking into account legacy systems data in the form of power flows. These are a few examples of how PMU systems promoted new methods to analyze and actuate on the power grid [3], [4], [5].

A key enabler for the practical implementation of these PMU systems is the availability of a precise time reference. Time synchronization is critical for PMUs, since time offsets effect phase errors rendering the phasor data unreliable [6]. The logal positioning system (GPS) rises to the challenge, with an accurate time reference of Caesium clocks which is further refined by estimating PMU locations, and using them to compensate for the propagation delay between GPS transmitters and receivers.

Due to the relevance of the information received from the PMUs, necessary to maintain the stability of an increasingly complex power grid, PMUs can not rely on GPS only whose control is outside the power utility. Furthermore, availability of the GPS time reference can be compromised by the reliability of GPS receivers connected to PMUs, or by fading and obstructions on GPS signals. Therefore, it is necessary to have

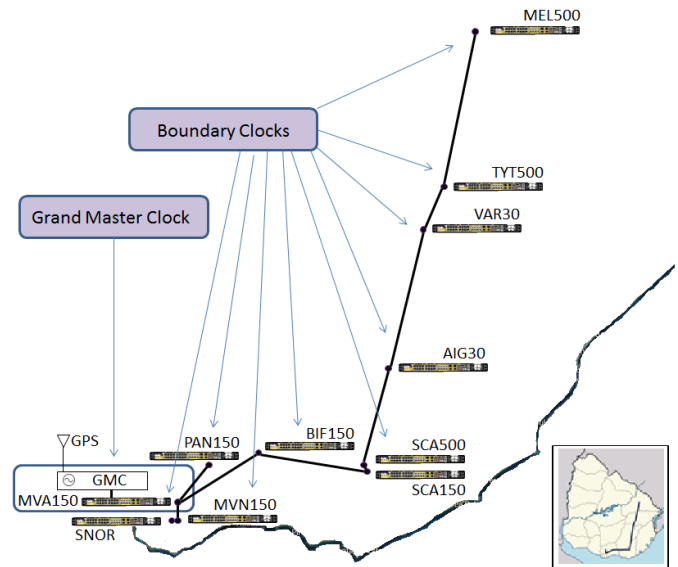


Fig. 1. Synchronization network deployed by the Information and Communications Technologies division at the Uruguayan power utility, UTE.

a backup synchronization system. One contingency solution for the GPS failure is to install an atomic clock at each station, extending run-time while GPS is not available. These clocks should not be autonomous, but need to be interconnected in order to be able to correct their time drift. For this reason UTE is developing the networked synchronization system described in this paper, as a GPS backup. Such a synchronization system is based on Precision Time Protocol (PTP) as it is defined in the IEEE Standard [7], and further refined for power system applications in the IEEE profile [8].

In this context, the goal of this paper is twofold. First to describe PTP and its implementation for the Uruguayan power grid, designed to provide time reference to $N_s \approx 100$ power sub stations (PSEs) of 150kV and 500kV, and hundreds of substations comprising the distribution system. The second goal is to advance a mathematical analysis of time offsets, describing their effect on PMU data noise, and the propagation of such a time-induced noise to the STE problem, both when STE relies on PMUs only [6], or when it takes into account nonlinear power flow measurements.

II. TIME PROPAGATION NETWORK

UTE is undergoing a modernization process for its 150kV and 500kV PSEs in order to render them compliant with the IEC 61850 Standard [9]. A remedial action scheme (RAS) is

[†]The authors are with the Information and Communications Technologies division of the Electric Power Company - UTE, Jujuy 2611, Montevideo, Uruguay; emails: {jbazerque, uribeiro, jcosta}@ute.com.uy

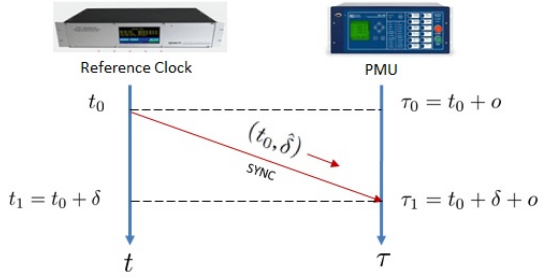


Fig. 2. Synchronization via Precision Time Protocol -Power Profile.

also being implemented, which connects PMUs and actuators with a centralized redundant control system.

In support for these developments, the Information and Communications Technologies division at UTE is implementing a nation-wide telecommunication network to communicate $N_s \approx 100$ PSEs, accounting for those already existent and those projected to connect new wind farms.

In addition to support IEC61850 and the RAS signals, the network will distribute time according to PTP - power profile. To this end, a Rubidium clock is located at a central point to act as a Grand Master Clock (GMC), connecting to GPS and propagating time information to all grid nodes. The GMC will provide a time reference signal that will be transmitted through a parallel communication network to be delivered at boundary clocks (BC) at the PSEs. The nodes for such a network, represented as black dots in Fig. 1, connect through fiber optic links with bandwidths of 100MB and 1GB per second, depicted as black lines. At the time of publication of this work, the system of $N = 11$ BCs depicted in Fig. 1 was implemented to synchronize the PSEs on the 500kV power line that interconnects the electric systems of Uruguay and Brazil. The length of the optical links vary from 400m for the link between MVN150 and SNOR to 114km from TYT500 to MEL500. Intermediate BCs were included in VAR30 and AIG30 in order to reduce the distance and guarantee connectivity of the optical links.

The BC is the device that acts as an interface between the nation-wide network and the local network inside each PSE. It must provide a time reference to the PSE clock, synchronized with the GMC and GPS. This time reference will be used as a backup in case the GPS signal is not available. For this project the BC is implemented by a network switch, compliant with the IEC 61850-3 standard on rugged design for operation in a PSEs, and with the PTP profile [8] for power applications.

III. PRECISION TIME PROTOCOL - POWER PROFILE

IEEE standard 1588 v2, 2008 [7] defines Precision Time Protocol (PTP), which provides a mechanism to estimate and correct the time offset, denoted as o , between a GMC and the time run by the internal clock of a PMU (or a BC). According to PTP, an estimate of the offset o is obtained by transmitting synchronization messages across a packet based telecommunication network connecting the GMC with the PMU. With the goal of computing the estimate $\hat{o} = o + e_o$,

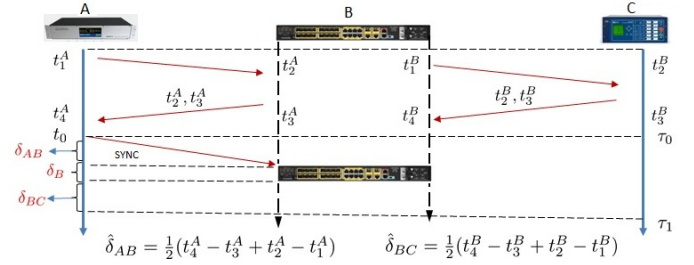


Fig. 3. PTP devices computing the estimate of the network propagation delay.

which approximates o up to an error level e_o , a synch message is transmitted by the GMC as depicted in Fig. 2. The time t_0 when the synch message is injected to the network is recorded by the GMC, and it is sent in the synch message as a time stamp. The synch message also carries an estimate $\hat{\delta}$ of the communication delay δ , which is obtained as described below. When the PMU receives the synch message, it records the arrival time τ_1 according to its internal clock, and in observance of $\tau_1 = t_0 + \delta + o$ (see Fig. 2), computes

$$\hat{o} = \tau_1 - t_0 - \hat{\delta}, \quad (1)$$

Then the PMU utilizes \hat{o} to correct its internal clock. According to (1), the estimation of δ is key to PTP. The detailed procedure to find $\hat{\delta}$ is described in Fig. 3, with A and C representing the GMC and the PMU, respectively, and B a middle telecommunication switch. First, the GMC estimates the path delay δ_{AB} from itself (A) to the next node (B) by sending a path delay request that departs at time t_1^A and arrives at time t_2^A . Node B replies with a path delay reply, that departs at time t_3^A and arrives at t_4^A . Then it estimates

$$\hat{\delta}_{AB} = \delta_{AB} + e_{AB} = \frac{1}{2} (t_4^A - t_3^A + t_2^A - t_1^A) \quad (2)$$

Notice that the offset between A and B is irrelevant for the calculation in (2), since adding a time o^B to both t_2^A and t_3^A would not affect the result.

Once the GMC has measured the propagation delay to its next neighbor B , then it sends a synch message containing $\hat{\delta}$, and the time-stamp t_0 . The next communication node B measures the propagation delay δ_{BC} with the same procedure, and accumulates $\hat{\delta} = \hat{\delta}_{AB} + \hat{\delta}_{BC}$. Node B also measures the internal queuing and processing time δ_B that it takes to the synch message to travel across B . That is, $\delta_B = t_{out}^B - t_{in}^B$, with t_{in}^B and t_{out}^B denoting the arriving and departing time to and from B , respectively. Then the estimate $\hat{\delta}_B = \delta_B + e_B$ is added to $\hat{\delta} = \hat{\delta}_{AB} + \hat{\delta}_B + \hat{\delta}_{BC}$, and the synch message forwarded to the next node C carrying $\hat{\delta}$. In a more general setup with nodes $\{A, B, C, \dots, N\}$, this procedure is repeated by all nodes in the path between the GMC represented by A and the PMU represented by N , to obtain the overall estimate

$$\hat{\delta} = \delta_{AB} + \sum_{i \in \{B, C, \dots, N\}} \delta_i + \delta_{i, i+1}$$

Once the PMU receives the synch message containing t_0 and $\hat{\delta}$, it computes \hat{o} using (1), and corrects its internal clock by

$$\tau \leftarrow \tau - \hat{o}$$

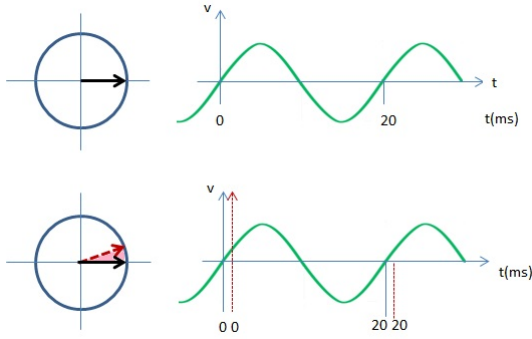


Fig. 4. Errors in phase measurements caused by synchronization offsets.

The function of a BC is also described in [7]. Set in between the GMC and the PMU, a BC acts as a proxy receiving the time reference from the GMC and acting itself as a GMC to the PMU side. Several BCs are placed on the path from MVA150 to MEL500 in the system of Fig. 1, propagating the GMC time reference to the PMUs at the connected PSEs.

The protocol is further defined for power system applications in the power profile IEEE C27 [8]. According to the normative appendix B in [8], the time offset must be estimated within a $1\mu s$ error across a network of up to $N = 16$ nodes between the GMC and the PMU. That implies that the telecommunication equipment comprising the nodes must be able to estimate the transit and propagation delay within an error level lower than $1\mu s/16$.

Remark 1 There are two main sources of error contributing to the error $dt = \hat{o} - o$ in the offset estimator. One is the hardware inaccuracy at setting the time stamps t_0 , τ_1 , and $\{t_{ia}, t_{id}\}_{i=1}^N$. The second one is caused by asymmetries between the forward and backward propagation paths between nodes, as they affect the propagation delay estimate in (2).

These sources of error are relatively small in magnitude, when compared to the propagation delay across the network, which typically amounts to 1ms-2ms over an optical fiber network. This would be the error if the time reference were distributed across the network without the PTP corrections.

The next section illustrates how a synchronization error dt across the network laying in the interval $(1\mu s, 1ms)$ translates to an error on the phase measured by a PMU.

IV. PHASE ERRORS CAUSED BY TIME OFFSETS

Fig. 4 shows two sine waves of frequency $f = 50\text{Hz}$ with the same phase $\theta = 0$, together with their phasor representations. The black phasors and blue graph axes represent these two waves as seen by an observer perfectly synchronized with a time reference. The red-dashed counterparts for the second sinusoidal represent the wave and its respective phasor as seen by an observer whose internal clock has a 1ms offset with respect to the time reference.

The phase deviation $d\theta$ in degrees varies linearly with the time mismatch dt measured in milliseconds according to

$$d\theta = 18(\text{deg}/\text{ms})dt. \quad (3)$$

Hence, two PMUs comparing the phase of line currents or bus voltages will incur in a error as in (3) when their internal clocks are out of synchronization with respect to each other.

How these time-induced errors propagate to state estimators is investigated next.

V. ERROR PROPAGATION IN LINEAR STATE ESTIMATION

One powerful feature of PMUs is that state estimation (SE) becomes a linear problem. Traditionally, the problem of SE implied solving for the magnitude and phase of all buses in the grid, from of voltage magnitudes and power flows at a set of measurement points. With $\mathbf{x} = (\bar{V}_i, \dots, \bar{V}_n)$ representing the vector of phasor-valued state variables and \mathbf{z} collecting network-wide data, the PSE problem entails solving

$$\mathbf{z} = \mathbf{h}(\mathbf{x}) + \mathbf{e}_z.$$

Since function $\mathbf{h}(\cdot)$ is nonlinear, typical estimation techniques would employ iterative methods in order to solve the (non-convex) least-squares estimation (LSE) problem,

$$\hat{\mathbf{x}} = \arg \min_{\mathbf{x}} \|\mathbf{z} - \mathbf{h}(\mathbf{x})\|^2, \quad (4)$$

or weighted versions of it.

PMU data are modeled as noisy versions of the current or voltage phasors in the network, which are related linearly through the network admittance matrix as in $\mathbf{I} = \mathbf{YV}$ [10, p.40], thus a linear measurement model follows (cf. \mathbf{H} in Example 1 below)

$$\mathbf{z} = \mathbf{Hx} + \mathbf{e}_z \quad (5)$$

with \mathbf{e}_z modeling measurement errors. For the purpose of the time sensitivity analysis here \mathbf{e}_z is decoupled in two terms

$$\mathbf{e}_z := \mathbf{e}_z^{(sync)} + \mathbf{e}_z^{(acc)} \quad (6)$$

to separate errors caused by faulty synchronization $\mathbf{e}_z^{(sync)}$ from the intrinsic inaccuracy of PMUs $\mathbf{e}_z^{(acc)}$ (see e.g., [11]).

Only $\mathbf{e}_z^{(sync)}$ is considered henceforth, setting $\mathbf{e}_z^{(acc)} = 0$ and $\mathbf{e}_z = \mathbf{e}_z^{(sync)}$. To describe $\mathbf{e}_z = \mathbf{e}_z^{(sync)}$ in more detail, consider the case in which a PMU is perfectly synchronized and measures a voltage phasor $\bar{V} = Ve^{\theta}$, then the same PMU with a time offset dt will measure $\bar{V}(dt) = Ve^{\theta}e^{j2\pi f dt} = \bar{V}e^{j2\pi f dt}$. Hence the measurement error will amount to $\bar{e}_z = \bar{V}(dt) - \bar{V} = \bar{V}(1 - e^{j2\pi f dt})$, and for small enough offsets $dt \ll 1/2\pi f$ it can be approximated as $\bar{e}_z = (j2\pi f dt)\bar{V}$. Similarly, if the PMU measures current \bar{I} with an offset dt , then it will be affected by noise $e_z = (j2\pi f dt)\bar{I}$. Collecting \bar{e}_z from all PMUs it follows that the error caused by time offsets takes the form

$$\mathbf{e}_z = (j2\pi f)\mathbf{D}dt \quad (7)$$

where dt is the vector of time offsets, and the diagonal matrix $\mathbf{D} := \text{Diag}(\mathbf{Hx}) \simeq \text{Diag}(\mathbf{z})$ contains noise-free versions of phasors measured by the PMUs. The mean and covariance matrix of \mathbf{e}_z take the form

$$E[\mathbf{e}_z] := (j2\pi f)\mathbf{D}dt \quad (8)$$

$$\mathbf{C}_z := E[\mathbf{e}_z\mathbf{e}_z^*] = -(2\pi f)^2\mathbf{D}\mathbf{C}_t\mathbf{D} \quad (9)$$

with $\mathbf{C}_t := E[\mathbf{d}t\mathbf{d}t^*]$ representing the covariance matrix of the time offsets.

Under this model, the LSE for \mathbf{x} in (5) takes the form

$$\hat{\mathbf{x}} = \arg \min_{\mathbf{x}} \|\mathbf{z} - \mathbf{H}\mathbf{x}\|^2 = (\mathbf{H}^*\mathbf{H})^{-1} \mathbf{H}^*\mathbf{z}. \quad (10)$$

where $(\cdot)^*$ represents the Hermitian transformation.

The estimator relates linearly to the data in (10) so that errors propagate linearly as well, and therefore the mean $\mathbf{E}_{\mathbf{d}x} := E[\hat{\mathbf{x}}(dt) - \hat{\mathbf{x}}]$ and covariance matrix $\mathbf{C}_{\mathbf{d}x} := E[(\hat{\mathbf{x}}(dt) - \hat{\mathbf{x}})(\hat{\mathbf{x}}(dt) - \hat{\mathbf{x}})^*]$ take the form

$$\mathbf{E}_{\mathbf{d}x} = (\mathbf{H}^*\mathbf{H})^{-1} \mathbf{H}^* E[\mathbf{e}_z] \quad (11)$$

$$\mathbf{C}_{\mathbf{d}x} = (\mathbf{H}^*\mathbf{H})^{-1} \mathbf{H}^T \mathbf{C}_z \mathbf{H}^* (\mathbf{H}^*\mathbf{H})^{-1} \quad (12)$$

Substituting (8) and (9) in (11) and (12), it follows

$$\mathbf{E}_{\mathbf{d}x} = (j2\pi f) (\mathbf{H}^*\mathbf{H})^{-1} \mathbf{H}^* \mathbf{D} E[\mathbf{d}t] \quad (13)$$

$$\mathbf{C}_{\mathbf{d}x} = -(2\pi f)^2 (\mathbf{H}^*\mathbf{H})^{-1} \mathbf{H}^* \mathbf{D} \mathbf{C}_t \mathbf{D} \mathbf{H}^* (\mathbf{H}^*\mathbf{H})^{-1} \quad (14)$$

Anticipating the next section, consider partitioning \mathbf{z} in two sub-vectors \mathbf{z}_a and \mathbf{z}_b , partitioning \mathbf{H} and \mathbf{C}_z accordingly. Then if \mathbf{z}_a and \mathbf{z}_b are independent \mathbf{C}_x can be decomposed as

$$\mathbf{C}_x := \mathbf{A} (\mathbf{H}_a^T \mathbf{C}_{z_a} \mathbf{H}_a + \mathbf{H}_b^T \mathbf{C}_{z_b} \mathbf{H}_b) \mathbf{A}^* \quad (15)$$

$$\mathbf{A} := (\mathbf{H}_a^T \mathbf{H}_a + \mathbf{H}_b^T \mathbf{H}_b)^{-1} \quad (16)$$

Remark 2 The structure of \mathbf{C}_t and \mathbf{C}_z depends on the connection of the BCs in the PTP network. If time offsets dt_i are independent one each other, then these matrices will be diagonal, but independence is implausible given the PTP network connections. For instance, if the BC at the PSE labeled SCA500 in Fig. 1 generates an error dt_{SCA500} then errors dt_{TYT500} and dt_{MEL500} at PSEs upstream will depend on dt_{SCA500} . A block diagonal structure can be assumed if the error at the central node can be neglected and the offsets of two network branches are assumed independent. In Fig. 1 dt_{MVA150} should be negligible to ensure that dt_{MVN150} and dt_{SNOR} to be independent of the offsets in the branch to PSE MEL500. Yet a more accurate model is a Markov Graph where nodes are assumed conditionally independent [12, pp. 627-631]. Under such a model, and if offsets can be modeled as Gaussian, the (i, j) entry of \mathbf{C}_t^{-1} will be null if offsets dt_i and dt_j are independent conditioned on all other offsets.

Remark 3 Upon knowing $E[\mathbf{d}t]$, the PTP mechanism in Fig (3) has the option to remove such a bias. That is why variances and not bias are critical in the analysis of this section.

Remark 4 A weighted version of the estimator can be considered by substituting $\|\mathbf{W}^{1/2}(\mathbf{z} - \mathbf{H}\mathbf{x})\|^2$ for the cost in (10), with \mathbf{W} defined as a diagonal matrix of weights for scaling and prioritizing. The simpler notation in (10) will be considered henceforth without loss of generality, since \mathbf{W} may be absorbed by redefining $\mathbf{H} = \mathbf{W}^{1/2}\mathbf{H}$ and $\mathbf{z}\mathbf{W}^{1/2}\mathbf{z}$.

Remark 5 All results in this section carry over by adding the mean and covariance of $\mathbf{e}_z^{(acc)}$, if not null, to (8) and (9).

Example 1 In order to build an instance of the model matrix \mathbf{H} , consider the case in Fig. 5 in which one wants to estimate the voltage phasor \bar{V}_0 (magnitude and angle) at bus $b = 0$, as a combination of the voltage phasors of all buses connected to $b = 0$. If these connected buses are numbered $b = 1, \dots, n$,

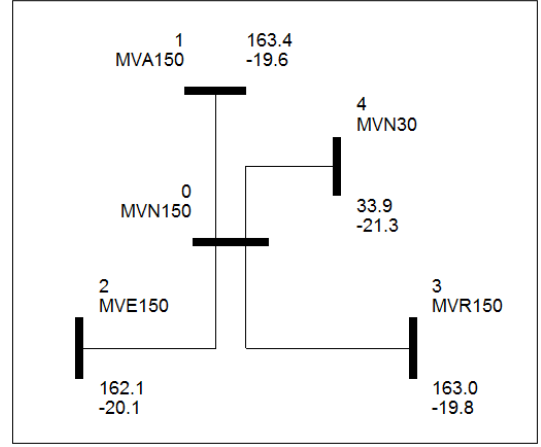


Fig. 5. Estimation of phasor \bar{V}_0 from PMU data collected at connected buses

then $\bar{z}_i = \bar{V}_i + \bar{e}_i$, $i = 1, \dots, n$; that is, each complex element of \mathbf{z} is a noisy measurement of the bus voltage phasor. The load at bus $b = 0$ is approximated as a constant admittance, and then absorbed in the admittance matrix model, hence voltage phasors satisfy $\sum_{i=0}^n \bar{Y}_{0i} \bar{V}_i$. Moving \bar{V}_n to the left hand side and substituting in $\bar{z}_n = \bar{V}_n + \bar{e}_n$ it follows

$$\begin{aligned} \bar{z}_i &= \bar{V}_i + \bar{e}_i, \quad i = 1, \dots, n-1 \\ \bar{z}_n &= -\sum_{i=0}^{n-1} \frac{\bar{Y}_{0i}}{\bar{Y}_{0n}} \bar{V}_i + \bar{e}_n \end{aligned} \quad (17)$$

which can be written as in (5) with $\mathbf{x} := \bar{V}_0, \dots, \bar{V}_{n-1}$ being the vector of voltage phasors to solve for, and \mathbf{H} is defined accordingly. In this case matrix \mathbf{H} is square and the LSE reduces to

$$\hat{\mathbf{x}} = \mathbf{H}^{-1} \mathbf{z}. \quad (18)$$

Extra equations can be added if the currents flowing on the lines reaching bus $b = 0$ are also sampled by PMUs. In that case $\bar{z}_{n+i} = \bar{I}_{i0} + \bar{e}_{n+i}$ so that the new measurements relates to the same n unknowns in (17)

$$\begin{aligned} \bar{z}_{n+i} &= \bar{Y}_{0i}(\bar{V}_i - \bar{V}_0) + \bar{e}_{n+i}, \quad i = 1, \dots, n-1 \\ \bar{z}_{2n} &= \bar{Y}_{0n} \left(-\sum_{i=0}^{n-1} \frac{\bar{Y}_{0i}}{\bar{Y}_{0n}} \bar{V}_i - \bar{V}_0 \right) + \bar{e}_{2n} \end{aligned}$$

and the system becomes overdetermined.

VI. MIXED LINEAR-NONLINEAR STATE ESTIMATION

Before the deployment of PMUs, the measurement vector \mathbf{z} consisted of active and reactive power flows injected to buses together with current and voltage magnitudes at these buses. These data were collected at remote terminal units (RTUs) without precise time information. As PMUs are deployed, phase angle differences are provided together with a time-stamp. Thus, an enabling problem to solve for the concurrence of the RTU and PMU technologies is the synchronization of all measurements across the network. In particular [3], [4] explore the problem of using such hybrid data for the SE problem. The goal of this section is to determine how errors in

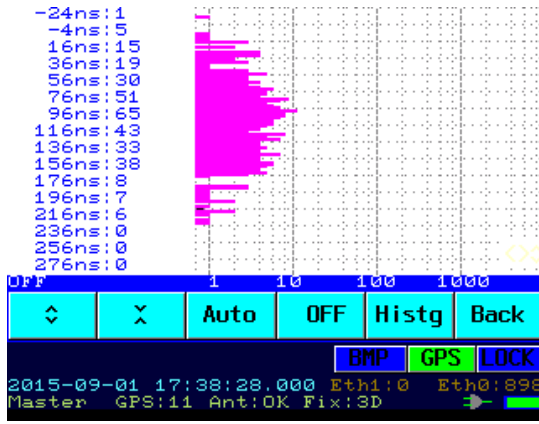


Fig. 6. Synchronization measurements.

synchronization affect the PSE problem when PMU readings are combined with legacy RTU data.

In this case the measurement model consists of both linear and nonlinear equations, for the PMUs and RTUs data respectively. Upon partitioning the measurement vector \mathbf{z} in two sub-vectors \mathbf{z}_{RTU} and \mathbf{z}_{PMU} , the measurement model becomes (cf. h_{RTU} given in Example 2)

$$\begin{aligned} \mathbf{z}_{\text{PMU}} &= \mathbf{H}_{\text{PMU}}\mathbf{x} + \mathbf{e}_{\text{PMU}} \\ \mathbf{z}_{\text{RTU}} &= \mathbf{h}_{\text{RTU}}(\mathbf{x}) + \mathbf{e}_{\text{RTU}}, \end{aligned} \quad (19)$$

The least-squares estimator becomes

$$\hat{\mathbf{x}} = \arg \min_{\mathbf{x}} \|\mathbf{z}_{\text{RTU}} - \mathbf{h}(\mathbf{x})\|^2 + \|\mathbf{z}_{\text{PMU}} - \mathbf{H}\mathbf{x}\|^2 \quad (20)$$

which can be solved by Gauss-Newton [12, p.391] method and the estimator covariance matrix becomes

$$\begin{aligned} \mathbf{C}_x^{GN} &:= \mathbf{A} (\mathbf{H}_{\text{PMU}}^T \mathbf{C}_{\text{PMU}} \mathbf{H}_{\text{PMU}} + \mathbf{J}_{\text{RTU}}^T \mathbf{C}_{\text{RTU}} \mathbf{J}_{\text{RTU}}) \mathbf{A}^* \\ \mathbf{A} &:= (\mathbf{H}_{\text{PMU}}^T \mathbf{H}_{\text{PMU}} + \mathbf{J}_{\text{RTU}}^T \mathbf{J}_{\text{RTU}})^{-1} \end{aligned} \quad (21)$$

with \mathbf{J}_{RTU} denoting the Jacobian matrix of $\mathbf{h}_{\text{RTU}}(\mathbf{x})$ with respect to \mathbf{x} , and \mathbf{C}_{RTU} and \mathbf{C}_{PMU} the covariance matrices for the error vectors \mathbf{e}_{RTU} and \mathbf{e}_{PMU} , respectively.

Comparing (15) to (21) when the set of PMU measurements \mathbf{z}_b is substituted by \mathbf{z}_{RTU} , it is apparent that \mathbf{J}_{RTU} and \mathbf{C}_{RTU} substitute \mathbf{H}_b and \mathbf{C}_{z_b} , and the contribution \mathbf{C}_{z_a} of the remaining set of PMUs carries over to \mathbf{C}_x^{GN} .

Example 2 Suppose that a PMU is not available at bus $b = 1$ in Example 1. Data from the removed PMU was two-dimensional so it should be replaced by two one-dimensional measurements. Let z_{1V} measure the voltage magnitude at bus $b = 1$, and z_{1I} the magnitude of the current flowing from $b = 1$ to $b = 0$. Then it is possible to write two nonlinear equations $z_{1V} = h_{1V}(\bar{V}_1) + e_{1V}$ and $z_{1I} = h_{1I}(\bar{V}_1, \bar{V}_0) + e_{1I}$ such that

$$h_{1V}(\bar{V}_0) := V_1 = \sqrt{\bar{V}_1 \bar{V}_1^*} \quad (22)$$

$$h_{1I}(\bar{V}_0, \bar{V}_1) := I_{10} = \sqrt{\bar{Y}_{10}(\bar{V}_1 - \bar{V}_0) \bar{Y}_{10}^*(\bar{V}_1 - \bar{V}_0)^*} \quad (23)$$

where $(\cdot)^*$ denotes conjugation.

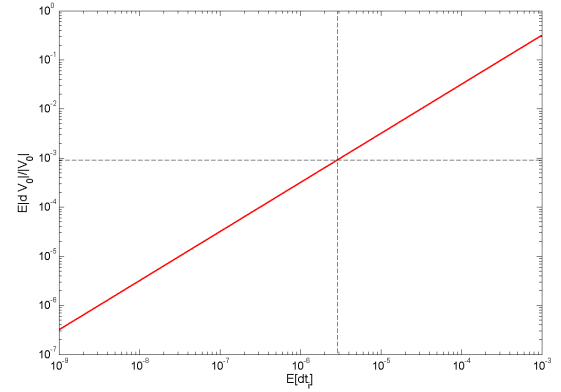


Fig. 7. Time-induced error in linear state estimation.

VII. NUMERICAL AND FIELD TESTS

This section describes the synchronization measurements performed on the PTP network, and explores the incidence on SE through numerical tests on the Uruguayan power grid.

A. Synchronization measurements

A field test was performed on the path of PTP nodes with four communication hops from the GMC in PSE MVA150 to the BC at node SNOR, with two intermediate BCs at MVA150 and MVN150 as depicted in Fig. 1. An offset analyzer, specially designed to measure time differences in the order of nanoseconds, is connected to the BC at SNOR. The analyzer compares the time stamp that receives from the BC at SNOR and to a time reference obtained directly through its local connection to GPS, computing the difference dt . Neglecting the difference between the GPS references obtained by the analyzer and the GMC, the difference dt renders equal to the PTP offset between the GMC and the BC at SNOR. A histogram for dt is shown in Fig. 6 with an average of 102.5ns and a standard deviation of 50ns .

B. State estimation

The state estimator described in Example 1 is numerically tested with real data from the Uruguayan power grid \mathcal{G} . With bus $b = 0$ in Fig. 5 representing the bus at the PSE MVN150, voltage \bar{V}_0 is estimated from PMU data collected at the buses $b = 1, \dots, 4$ directly connected to it. Data \mathbf{z} is not obtained directly from the PMUs, but simulated by solving the power flow problem over the whole grid.

The first equation in (18) gives the desired estimate \hat{V}_0 for the voltage phasor at bus $b = 0$, that is

$$\hat{V}_0 = - \sum_{i=1}^n \frac{\bar{Y}_{0i}}{\bar{Y}_{00}} \bar{V}_i^{\text{PMU}} \quad (24)$$

Let $\hat{V}_0^{(\text{offset})}$ denote the estimator that is obtained by substituting $\bar{V}_i^{\text{PMU}} \exp(2\pi f dt_i)$ for \bar{V}_i^{PMU} in (24), in account for time offsets dt_i , $i = 1, \dots, n$ in the data.

Errors dV_0 are then computed as the magnitude of the difference between $\hat{V}_0^{(\text{offset})}$ and \hat{V}_0 . Fig. 7 depicts the mean

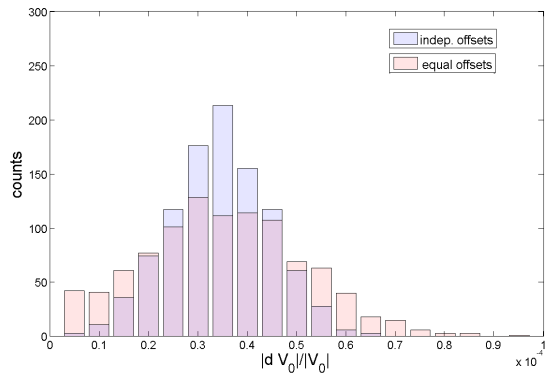


Fig. 8. Relative errors in state estimation produced by the variability of the PMU time reference.

of dV_0 , that is $E[\hat{V}_0^{(\text{offset})} - \hat{V}_0]$ as a function of the mean offset $E[dt_i]$ in the range 1ns to 1ms. A worst-case scenario is considered for this curve, in which all offsets coincide, that is $E[dt_1] = E[dt_2] = \dots = E[dt_n]$ hence they have the same sign, not canceling one each other in (24).

It is reflected in Fig. 7 that offsets close to 1ms are not admissible, since they effect errors on the order of 30 percent in SE, while time errors in the range of a few μs keep relative estimation errors in the order of 10^{-3} . The horizontal dashed line in Fig. 7 represent $E(e_z^{(\text{acc})})$ in (6) as reported in [11], and the corresponding vertical line at $E[dt_i] = 3.1\mu\text{s}$ indicates the time offset such that the corresponding $E[dx]$ is comparable with the intrinsic inaccuracy of the PMU.

Regarding the variability of the result, Fig. 8 depicts the histograms of the relative error of $d\bar{V}_0$ for the cases discussed in Remark 2. The blue histogram corresponds to the case in which all offset are equal. In the case when time offsets are independent, the law of large number acts to reduce the variance of the estimator, as shown in the red histogram. Fig. 9 compares these errors to the PMU inaccuracy level.

VIII. CONCLUSIONS

A time distribution protocol was implemented to carry time information across the power grid, providing a backup for the GPS reference. Path delays of a few milliseconds are typically found over wide area communication networks connected by fiber optics. If a time stamp sent through the network is not corrected for this delay, then the time offset apparent at two buses is reflected as a spurious phase deviation in the PMU data collected at these buses. When PMU data from different buses are combined across the network, faulty synchronization may render it useless. Specifically, the state estimation experiments carried out numerically in section VI show that the effect of 1 millisecond offset could add up to 30-percent error in the magnitude of the estimated voltages. Implementing the precision time protocol version for power applications it was possible to reduce these offsets to less than one microsecond according to field measurements, and the state estimator is improved to attain a relative error lower than the PMU intrinsic inaccuracy.

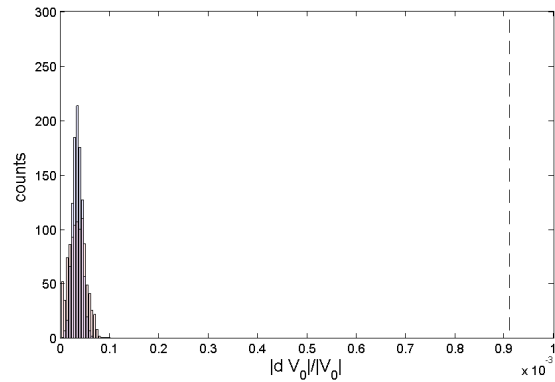


Fig. 9. Comparison of synchronization errors to PMU intrinsic inaccuracy.

IX. ACKNOWLEDGEMENTS

The authors want to thank multiple actors at UTE that assisted to this work. Alejandro Becv, Jose Luis Barattini, Sebastian Fernandez, and Pablo López provided the connection to the GMC and performed offset measurements. Mateo Ruétalo supported this project and helped with the set up of a synchronization lab. Pablo Pena provided the power grid data used in numerical experiments. Nicolás Francia, Florencia Mainnenti, Pablo Bethencourt, Diego Faral, and Sonia Schatz installed equipment comprising the PTP network. Alejandro Cavalli, Mariana Riera, Tania Díaz, and Gonzalo Borowski assisted with and provided data about the fiber optics network connecting the BCs.

REFERENCES

- [1] A. G. Phadke and J. S. Thorp *Synchronized phasor measurements and their applications*, Springer, 2008.
- [2] C.W. Liu and J.S. Thorp "New methods for computing power system dynamic response for real-time transient stability prediction" *IEEE Circuits and Systems I: Fundamental Theory and Applications*, 2000
- [3] Ming Zhou; V. A. Centeno, J.S. Thorp, and A.G. Phadke, "An Alternative for Including Phasor Measurements in State Estimators," *IEEE Trans. on Power Systems*, vol.21, no.4, pp. 1930-1937, Nov. 2006.
- [4] A. Gomez-Exposito, A. Abur, P. Rousseaux, A. d. I. V. Jaen, and C. Gomez-Quiles, "On the use of PMUs in power system state estimation," in *Proc. 17th Power Sys. Comp.*, Stockholm, Sweden, Aug. 22-26, 2011.
- [5] J. Lavaei and S. H. Low, "Zero duality gap in optimal power ow problem," *IEEE Trans. on Power Systems*, vol. 27, no. 1, pp. 92107, Feb. 2012.
- [6] Peng Yang, Zhao Tan, A. Wiesel, and A. Nehorai, "Power System State Estimation Using PMUs With Imperfect Synchronization," *IEEE Trans. on Power Systems*, vol.28, no.4, pp. 4162-4172, Nov. 2013.
- [7] The IEEE Precise Networked Clock Synchronization Working Group *IEEE 1588 Standard for A Precision Clock Synchronization Protocol for Networked Measurement and Control Systems* IEEE, 24 July 2008.
- [8] IEEE 1588 Profile for Protection Applications Working Group *IEEE PC37.238 Standard Profile for Use of IEEE 1588 Precision Time Protocol in Power System Applications*, IEEE 2011.
- [9] J. McGhee and M. Goraj, "Smart High Voltage Substation Based on IEC 61850 Process Bus and IEEE 1588 Time Synchronization," in *Proc. First IEEE International Conference on Smart Grid Communications*, pp. 489,494, 4-6 Oct. 2010.
- [10] P. M. Anderson and A. A. Fouad, *Power System Control and Stability*, 2nd Ed. IEEE Press NJ, 2003.
- [11] Z. Huang, T. Faris, K. Martin, J.F. Hauer, C.A. Bonebrake, and J.M. Sha "Laboratory Performance Evaluation Report of SEL 421 Phasor Measurement Unit," National Technical Information Service, U.S. Department of Commerce, Dec. 2007.
- [12] T. Hastie, R. Tibshirani, and J. Friedman, *The Elements of Statistical Learning* 2nd Edition Springer, 2009.